Review

Israel Journal of Chemistry
www.ijc.wiley-vch.de

doi.org/10.1002/ijch.202300077

Calix[5]arene Self-Folding Cavitands: a New Family of Bio-Inspired Receptors with Enhanced Induced Fit Behavior

Rubén Álvarez-Yebra[+],[a] Ricard López-Coll[+],[a] Núria Clos-Garrido,[a] David Lozano,*[a] and Agustí Lledó*[a]

Dedicated to Prof. Julius Rebek on occasion of the 2023 C. David Gutsche Award recognition.

Abstract: Self-folding cavitands represent the quintessential form of bioinspired synthetic receptors, featuring deep hydrophobic cavities that engage in host-guest chemistry reminiscent of that operating in biomolecules. Although remarkable proof-of-concept applications have been reported, the narrow and rigid spaces of the legacy resorcin[4]arene derived hosts constitute a liability towards the development of specific applications in catalysis, sensing or sequestration. While notable efforts to expand the size of the cavities have been reported, the development of confined spaces reproducing the highly adaptable nature of biological receptors is a largely unaddressed issue. This review summarizes the development of a new family of calix[5]arene derived self-folding cavitands displaying enhanced induced fit and conformational selection phenomena. Our approach capitalizes on hydrogen bonding preorganization rather than the covalent restriction approaches customary of conventional supramolecular chemistry.

Keywords: Cavitands · Host-guest systems · Molecular recognition · Calixarenes · Induced fit

1. Introduction

The mimicry of biological host-guest behavior is the foundational motivation of supramolecular chemistry.[1] Since the emergence of this field in the 1970s, the imagination and creativity of chemists has fostered the appearance of thousands of examples of molecular encapsulation by synthetic receptors of diverse shapes, sizes and typology.[2] Calixarenes[3] and resorcinarenes[4] have enjoyed enormous popularity as starting scaffolds for molecular receptors, because the pre-organized concave shapes of these macrocycles make them ideal for building up deeper hydrophobic concavities. In 1982, Cram first coined the term *cavitand* to describe *"synthetic organic compounds that contain enforced cavities large enough to accommodate simple molecules or ions"*.[5] In the context of modern supramolecular chemistry, this somewhat generic definition could be applied to a plethora of different hosts assembled by assorted methods. But since its inception, the term *cavitand* has been applied almost exclusively to resorcin[4]arene (**R4A**) derived hosts (**1**-**2**, Figure 1).[6] For the sake of simplicity, we will use the term "**R4A** derived cavitands" throughout this review to refer to monomeric hosts obtained by expansion of **R4A** with aromatic units through S_NAr condensation reactions of the phenolic functions. Such receptors have some distinct features, namely, a cylindrical cavity that is sealed at one end and open at the other, and a fluxional behavior that allows the host to switch from the closed conformer (*vase*) to an open one (*kite*), allowing the release of guests within.[7] The original concept was further refined by Rebek with the introduction of *self-folding cavitands* (**2**), featuring adjacent secondary amide groups at the rim.[8] These amides engage in a cooperative hydrogen bond network that stabilizes the vase conformer, increasing the barriers of the vase-kite transition and slowing down guest exchange in turn. The platform devised by Rebek allows functionalization of one of the cavitand's wall, giving rise to the development of interesting applications such as the isolation of reactive intermediates or the development of bioinspired and supramolecular catalysis.[9] Despite all these feats, we identified some downsides of the **R4A** derived self-folding cavitands that limit the development of new and meaningful applications, specifically in the area of catalysis. First, the binding space of these cavitands is relatively reduced, limiting the choice of guests to small molecules and substrates of limited relevance. And second, and most important, the binding space of **R4A** self-folding cavitands is rather rigid, severely limiting the emergence of induced-fit and conformational selection phenomena that are central to the outstanding capabilities of biological receptors (proteins and enzymes).[10] This statement may sound controversial in light

[a] *R. Álvarez-Yebra,[+] R. López-Coll,[+] N. Clos-Garrido, Dr. D. Lozano, Dr. A. Lledó*
Institut de Química Computacional i Catàlisi (IQCC), Universitat de Girona
Maria Aurèlia Capmany 69, 17003, Girona, Spain
E-mail: agusti.lledo@udg.edu
davidlozanomena@gmail.com

[+] *These authors contributed equally*

of previous claims of induced fit behavior in **R4A** derived cavitands,[11] but our own Molecular Dynamics (MD) simulation studies on this matter eloquently reveal that the flexibility of these receptors is far removed from the plasticity displayed by enzymes and proteins.[12] Accordingly, we envisaged the development of a completely new family of self-folding receptors with expanded binding spaces displaying genuine induced fit behavior, which should facilitate the development of applications with a wider and more significant range of guests and substrates. This account summarizes our efforts in this direction to develop new calix[5]arene (**C5A**) derived self-folding cavitands, with an emphasis on the design rationale.[13]

2. Cavitand Design

At the onset of this project, we focused our attention on expanding the volume of the binding site. Although notable efforts have been made by prominent research groups to make cavitands with expanded cavities, the majority of these efforts are focused on expanding **R4A**-derived structures along the longitudinal dimension, providing longer albeit equally narrow confined spaces.[14] A logical step forward from previous efforts was to use a resorcin[5]arene (**R5A**) as supporting scaffold, an approach that has important limitations. On one hand, synthetic access to **R5A** is not trivial, despite recent advances, and securing useful quantities of **R5A** precursors for further development appeared as a daunting and time consuming task.[15] Secondly, the accessible **R5A** macrocycles so far reported feature methylene hinges between aromatic panels, rather than the typical methine substituents of **R4A** derivatives, a difference with deep implications in the conformational mobility of these macrocycles and hence their reactivity vis-à-vis to bridging reactions. In initial stages of this project, we found this flexibility to be critical for bridging processes based on S_NAr reactivity. When we attempted the cyclocondensation reaction of known *unsubstituted* **R4AH**[16] with

Rubén Álvarez-Yebra obtained his BSc (2017) and MSc (2018) from Universitat the Barcelona (Advisors: Prof. Jaume Granell, Prof. Xavier Verdaguer). He carried out his doctoral studies at Universitat de Girona under the supervision of Prof. Agustí Lledó, focusing on the design, preparation and study of calix[5]arene derived cavitand receptors.

Ricard López-Coll obtained his BSc (2018) and MSc (2019) from Universitat the Girona, under the supervision of Prof. Agustí Lledó. He is currently carrying out his PhD thesis in the same group, focusing on the rational design of functional cavitands. In 2022, he carried out a short research stay with Prof. Konrad Tiefenbacher (Universität Basel).

Núria Clos-Garrido studied chemistry at Universitat de Girona (2023), She carried out undergraduate work under the supervision of Dr. Agustí Lledó, and is currently an R+D intern at Givaudan.

David Lozano received his PhD in synthetic organic chemistry at Universitat de Barcelona (2017, Advisor: Prof. Pelayo Camps). He next shifted focus to apply his synthetic experience to the construction of supramolecular architectures. He carried out a first postdoctoral stage at Universitat de Girona under the supervision of Prof. Agustí Lledó, exploring the host-guest properties of expanded self-folding cavitands. He next joined the group of Prof. Steve Goldup at the University of Southampton, where he developed novel synthetic approaches to mechanically chiral interlocked molecules. Later on, David joined the group of Dr. Sander Wezenberg at Leiden University, developing applications of supramolecular stimuli-responsive systems in transmembrane-associated biological processes.

Agustí Lledó studied Chemistry at Universitat de Barcelona, where he received his PhD (2006) working on the development of the Pauson-Khand reaction and its synthetic applications. In 2007 he moved to The Scripps Research Institute to carry out post-doctoral research in the group of Prof. Julius Rebek Jr. Later on, he joined the Institute for Research in Biomedicine, Barcelona (IRB Barcelona) as a Juan de la Cierva research fellow (2010). In 2014, he relocated to Universitat de Girona as a Ramón y Cajal fellow, where he was promoted to Associate Professor in 2019. His research interests include supramolecular chemistry, synthetic organic chemistry and homogeneous catalysis.

Israel Journal of Chemistry

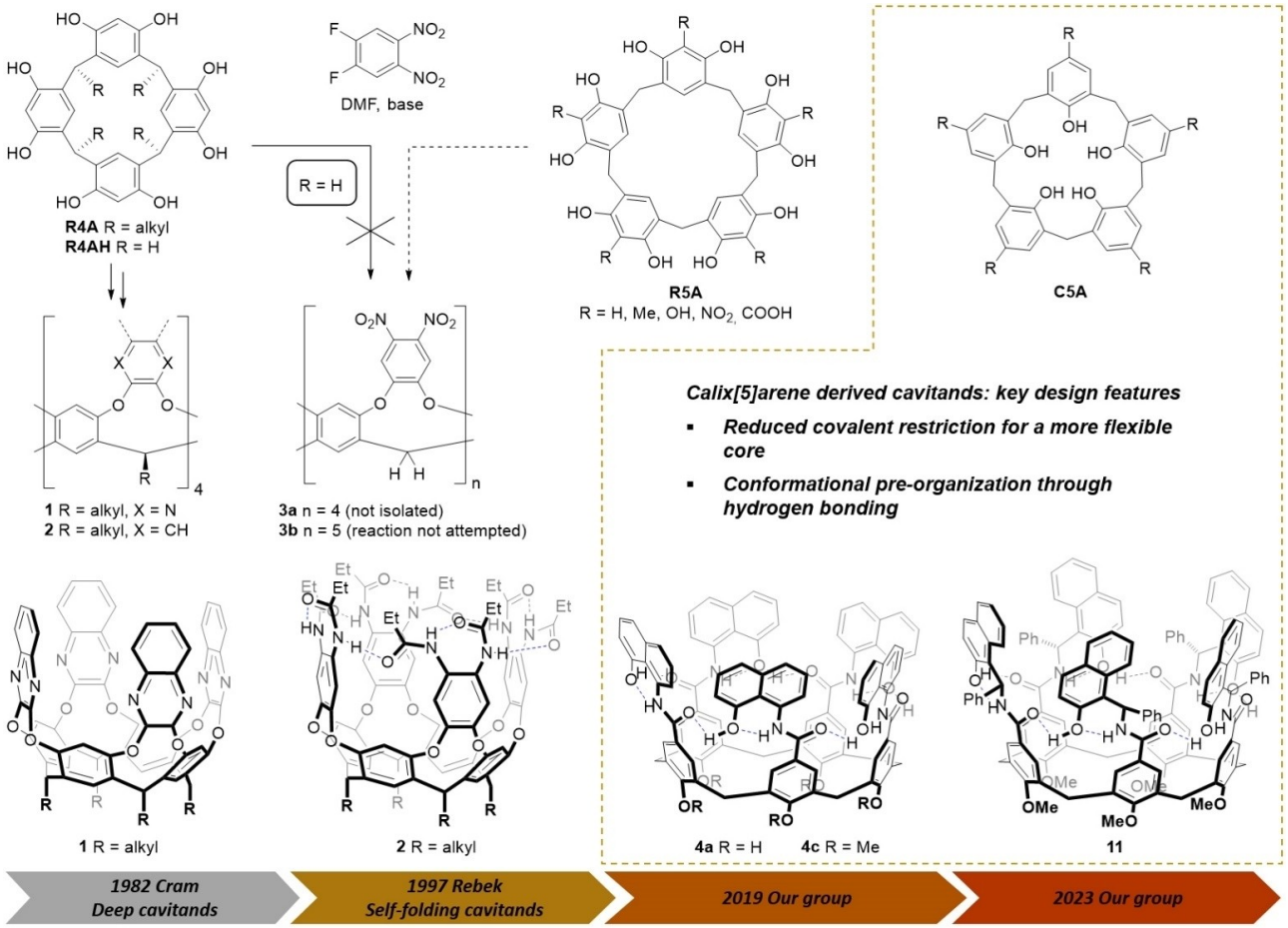

Figure 1. Evolution of the self-folding cavitand concept, from rigid cavities enforced by covalent bridging of **R4A** (**1**, **2**) to the more flexible structures derived from **C5A** and stabilized primarily by hydrogen bonding (**4a**, **4c**, **11**).

1,2-difluoro-4,5-dinitrobenzene, we were unable to isolate the desired octanitro cavitand **3a** despite many efforts, casting doubts on the viability of bridging the higher **R5A** analogue in a similar way to obtain **3b** (Figure 1). Recently, Tiefenbacher and co-workers have developed xanthene[n]arenes (n = 3, 4) and acridane[4]arenes, wider analogues of **R4A** that are rigid and well-suited for bridging by S_NAr condensation, giving access to cavitands of heightened dimensions.[17] Given our original motivation to build up new receptors based on non-covalent stabilization schemes, we considered whether the higher flexibility of calixarenes with methylene hinges could be used to our advantage. Rather than building up the cavitand by covalent bridging, establishing non-covalent linkages between the upper panels of a given receptor would allow to exploit the native flexibility of the supporting scaffold. This approach made the converging phenolic units of **R4A** and **R5A** unnecessary, and we therefore decided to explore **C5A** as a suitable supporting scaffold, a macrocycle that can be accessed with relative ease. Albeit low yielding, the protocols developed by calixarene pioneer C. David Gutsche and co-workers allow the preparation of multigram quantities of **C5A** in a single synthetic operation.[18] The exhaustive seminal studies by Gutsche and others on calixarene dynamics and conformational behavior where also key to our design choice, since **C5A** is the largest of the calix[n]arene congeners clearly favoring bowl-like conformers, which we deemed ideal for extension into deeper, preorganized cavities.[19] Since one **C5A** benzamide-type derivative had been previously documented,[20] we sought out to capitalize on the well-known proficiency of amide groups to establish cooperative hydrogen bond networks. This layout presented a major hurdle: amide groups positioned at the *para* positions of **C5A** are too distant to engage in hydrogen bonding (Scheme 1a). To overcome this limitation, we envisaged the preparation of amide derivatives bearing hydrogen bonding auxiliary groups that would establish a continuous, stabilizing network of cooperative hydrogen bonds. Our final objective was the stabilization (both kinetically and thermodynamically) of the resulting cavitand receptors in closed conformers defining deep concavities akin to the vase conformer characteristic of **R4A** derived cavitands. This new approach would provide, if successful, a much more flexible and adaptable space than that

Israel Journal of Chemistry

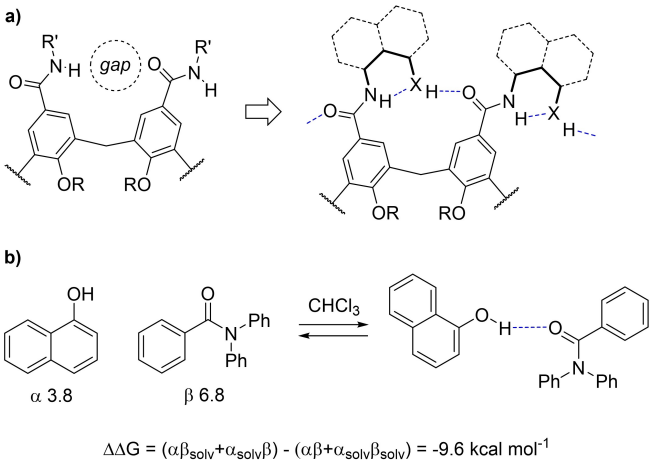

Scheme 1. a) Hydrogen bond auxiliary concept and b) intermolecular hydrogen bonding model.

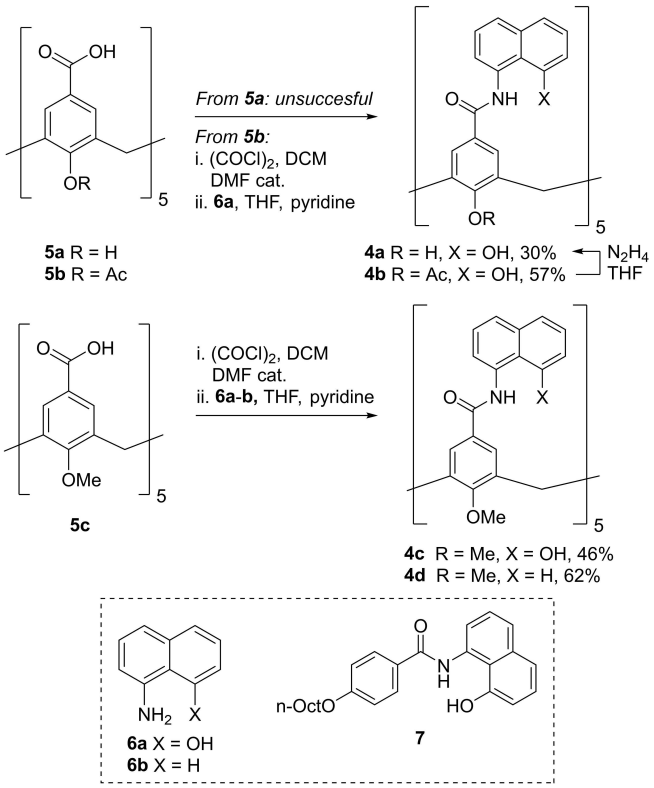

Scheme 2. Synthesis of cavitands **4a-d**. Inset: building blocks for the cavitands' upper panels (**6a-b**) and reference model compound **7**.

of **R4A** derived cavitands, since the envisaged **C5A** derived cavitands would feature only one *layer* of covalent restrictions –that of the **C5A** core structure–, relying entirely on hydrogen bonding to stabilize the closed conformer. Conversely, **R4A** derived cavitands have an additional layer of covalent restriction –the bridging upper aryl units. It is in fact the covalent structure of **R4A** type cavitands what dictates their essential conformational behavior, providing in turn a quite rigid scaffold of limited adaptability.

3. First Generation Cavitands

3.1. Cavitand Based on the Parent C5A and 1,8-Aminonaphthol (4a)

With all the previous design considerations in mind, we started this project by targeting cavitand structure **4a** featuring 1,8-amidonaphthol panels (Figure 1). Cavitand **4a** could be prepared by condensation of a **C5A** penta-acid building block (**5**)[13b,20] and readily available 1,8-aminonapthol (**6a**, Scheme 2).[13b,21] We rationalized that the phenol groups would enable the desired hydrogen bond seam along the mid-section of the cavitand. Based on well-established hydrogen bonding parameters α and β,[22] a favorable ΔG value can be calculated for the intermolecular interaction of *N*,*N*-diphenylbenzamide and 1-naphthol in $CHCl_3$, which serves as a model for the intramolecular interaction that is key for bridging the conformationally mobile upper panels of the cavitand (Scheme 1b). A positive cooperative effect can be anticipated in the cavitand structure due to hydrogen bonding from the neighbouring amide NH to the phenol group, adding up to the calculated stabilizing effect. In our first approximation, we intended to have free phenolic groups at the lower rim of the cavity, which would engage as well in hydrogen bonding adding to the overall stabilization of a wide and spherical deep cavity, as ascertained by DFT calculations. Attempts to perform direct coupling of penta-acid **5a** bearing free hydroxyl units were unsuccessful, due to the formation of complex mixtures of highly polar compounds. Eventually, we gained access to the desired cavitand **4a** by coupling of peracetylated penta-acid derivative **5b** and 1,8-aminonaphthol via the corresponding acyl chloride, and subsequent cleavage of the acetate groups in intermediate **4b** with hydrazine.

Cavitand **4a** turned out to be poorly soluble in the majority of conventional non-hydrogen bond competitive solvents, making it difficult to validate our initial hypothesis. Eventually, we found out that **4a** was soluble in *o*-dichlorobenzene-d_4 and tetrachloroethane-d_2. Gratifyingly, the features of the resulting ^{1}H NMR spectra indicated that **4a** was indeed stabilized by hydrogen bonding in a cone conformer that was kinetically stable in the NMR time scale, as inferred from the far downfield shifts of the NH and OH protons and, most importantly, the splitting of the **C5A** methylene bridge resonances into a pair of diastereotopic protons (Figure 2a). In addition to its limited solubility, cavitand **4a** was found to be somewhat unstable in solution, prompting us to look for alternative structures that would provide a more robust platform for investigating the folding process and host-guest behavior of the newfound cavitand scaffold. At this point, we reasoned that the more obvious choice would be to protect the phenolic groups at the lower rim of the cavitand to enhance

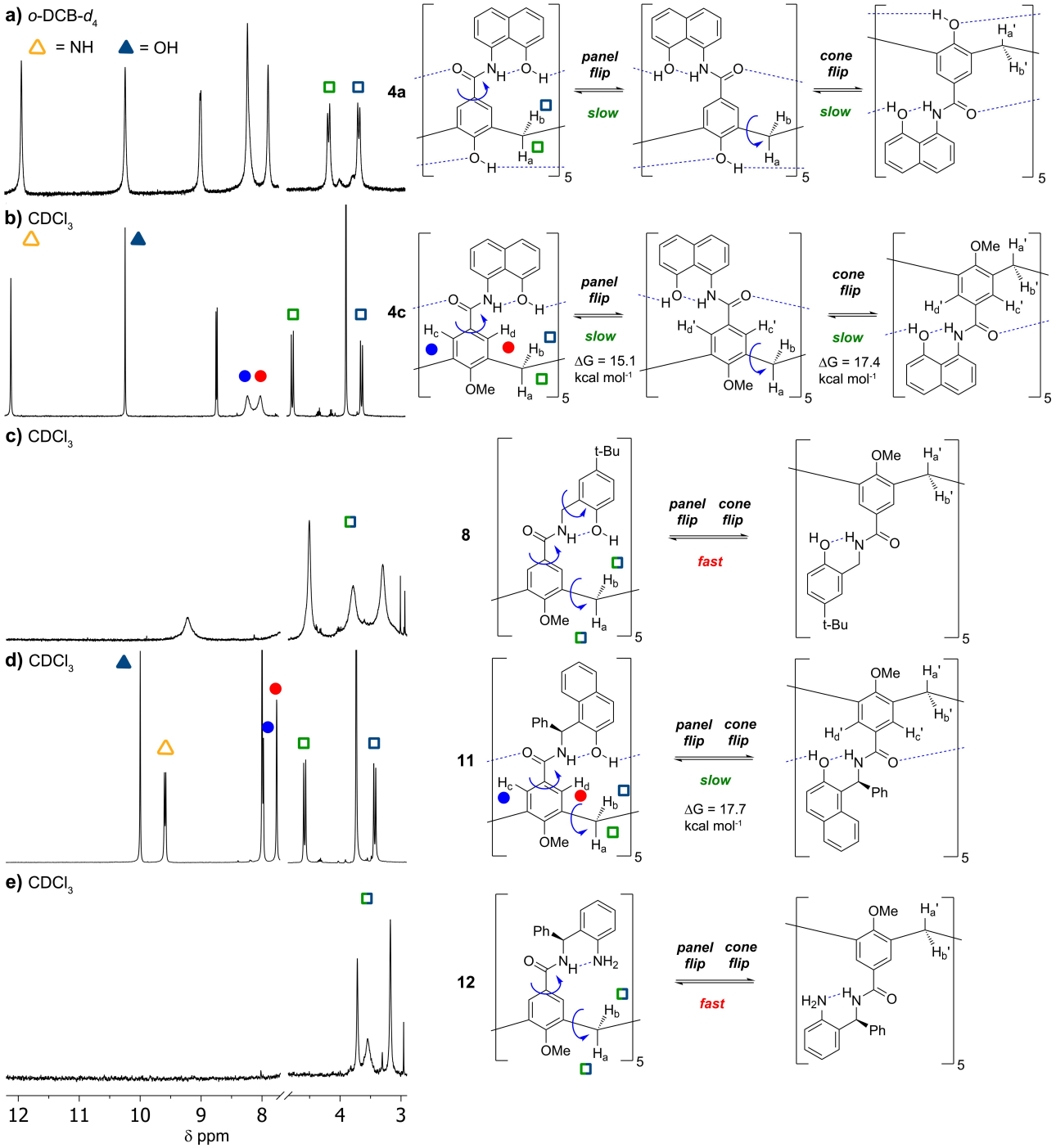

Figure 2. ^{1}H NMR spectra (selected regions) of cavitands a) **4a**, b) **4c**, c) **8**, d) **11** and e) **12**. Shown on the side for each case are the involved conformational exchange processes, including the associated barriers (ΔG) obtained from EXSY experiments.

solubility in low polarity organic solvents, a modification that would probably also result in higher stability towards oxidation of the **C5A** core.

3.2. Cavitand Based on Penta(*O*-Methyl)-C5A and 1,8-Aminonaphthol (4c)

On this regard, we envisioned that the previously reported *O*-permethylated **C5A** building block **5c** (Scheme 2) would match our aforementioned stability and solubility

considerations.[20] Cavitand **4c** was easily prepared via reaction of the penta-acid precursor **5c** with oxalyl chloride and a catalytic amount of DMF to form its acyl chloride derivative, and subsequent coupling with 1,8-aminonaphthol (**6a**) in good yield.[13b] Gratifyingly, **4c** could be obtained in good purity after flash column chromatography and was soluble in conventional non-hydrogen bonding solvents such as chloroform and dichloromethane.

With cavitand **4c** in hand, we firstly focused on investigating the conformational nature of the flexible synthetic receptor, aiming at assessing the stabilizing contribution of the H-bond network on sewing the cone shape of the cavitand. To do so, we run a series of 1D and 2D NMR spectroscopy experiments to properly characterize the conformation and chemical behavior of cavitand **4c** in solution. ^{1}H NMR experiments performed in DMSO-d_6 displayed **4c** as a D_{5h}-symmetry receptor due to the averaged resonances of aromatic protons of the **C5A** core, indicating that the hydrogen bond seam is breached by the solvent. Thus, the deuterated solvents for conformation and binding experiments had to be selected in order not to disrupt the crucial non-covalent linkage of the aromatic panels. NMR analysis in $CDCl_3$ revealed two separate resonances for the same aromatic protons (H_c/H_d, blue and red dots, Figure 2b), suggesting a slow rotation of the upper rim panels around the aryl–CO bond in the NMR time scale at 298 K. Besides, the presence of panel-linking H-bonds in cavitand **4c** was evidenced by the difference in the NMR shifts of the amido NH and naphthol OH resonances in comparison with its acyclic monomer **7** (Scheme 2). The OH proton signal in **4c** is shifted downfield ($\Delta\delta = 3.86$ ppm) with respect to **7**, indicating a strong H-bond contribution of the naphthyl OH groups in intramolecularly sewing the panels. Additionally, a considerable downfield shift is also observed in the case of the amide NH protons ($\Delta\delta = 0.82$ ppm). ^{1}H-NMR experiments at different concentrations were performed in order to evaluate whether self-aggregation was the cause of such shift on the proton signals. The OH and NH of cavitand **4c** resonances remain unaffected at different concentrations, ruling out the formation of aggregates as the cause of the signal shift. Regarding the cone inversion or "cone flip" motion of the **C5A** core (typically referred to as "cone-cone interconversion" in the specialized calixarene literature), ^{1}H NMR in $CDCl_3$ showed the distinct AB system of diastereotopic nuclei for the methylene protons H_a/H_b of **4c** (green and blue squares, Figure 2b) previously observed in **4a**, confirming that the receptor is able to stabilize an averaged C_5 symmetry cone conformation in solution through non-covalent bonding of the upper panels. Although efforts have been made in our lab to corroborate these structural hypotheses in the solid state by X-ray diffraction analysis, we have so far been unable to obtain suitable crystals of **4c** or any of the other cavitands herein reported.

A deeper understanding of conformational exchange of cavitand **4c** was gained using VT-NMR and EXSY analysis. The resonances for protons in exchange H_c/H_d at 298 K are broader compared to the ones for H_a/H_b, meaning that the aromatic panel rotation and the cone inversion occur at different rates. VT-NMR shows complete sharpening of the H_c/H_d pair at lower temperatures, whereas coalescence of these resonances was reached at temperatures higher than 325 K. 2D EXSY experiments in $CDCl_3$ confirmed chemical exchange between each of the above pairs of resonances, evidencing the existence of equilibriums in slow regime regarding the upper panel rotation and cone inversion. By integrating the cross peaks of the correlated signals, we could deduct the rate constants of the process and their associated energy barriers ($\Delta G^{\neq}$): barriers of 15.1 ± 0.2 kcal mol^{-1} for the panel rotation at 272.5 K, and ≥ 17.4 kcal mol^{-1} for the cone inversion at 299.3 K. These findings evidence the crucial contribution of the hydrogen bond seam in stabilizing the cone shape of cavitand **4c**, since a barrier below 9.3 kcal mol^{-1} was previously estimated for the cone inversion motion of the parent *O*-permethylated **C5A** core.[19b] The resulting stabilization energy ($\Delta\Delta G^{\neq} \geq 8.1$ kcal mol^{-1} in $CDCl_3$) is quite remarkable given the fact that it is accomplished by hydrogen bonding, rather than by covalent restriction as in **R4A** derived cavitands.

Preliminary modelling of cavitand **4c** by DFT optimization and molecular dynamics (MD) simulations depicted the synthetic receptor as a highly flexible cavity, featuring unusual shape adaptability upon accommodation of a guest. DFT minimization of the structure in the gas phase confirmed the highly stable cyclic cone-shaped receptor sewed by a hydrogen bond network, showing a flattened arrangement of the naphthalene panels through π-π stacking. MD simulations of **4c** (Section 5) corroborated the flexible nature of the cavitand with the ability to adopt several irregular vase-like shape structures. Panel flip and cone inversion conformational changes are not observed during the MD simulation in the time frame of study, in good agreement with the energy barriers calculated by NMR. The wide cavitand is able to accommodate up to four chloroform molecules within the cyclic walls of the receptor. However, the preferred flattened stacking of the upper aromatic panels suggested that **4c** could efficiently bind extended planar aromatic molecules, stabilized inside the cavity through π–π stacking interactions. Thus, we decided to experimentally study the binding of a wide range of commercially available planar polycyclic aromatic hydrocarbons (PAHs, **G1-G9**, Figure 3) by ^{1}H-NMR spectroscopy. Binding titrations of **G1-G7** in $CDCl_3$ upon addition of increasing amounts of the guests did not lead to any spectral change of the proton signals related to **4c**, suggesting no stabilization of the smaller PAHs of the series inside the cavitand. However, larger aromatic systems such as coronene (**G8**) and *N,N*-dimethylnaphthalenediimide (**G9**) were efficiently bound by cavitand **4c**, displaying significant shifts of the aromatic and methylene signals, strongly influenced by the presence of the guest. NMR titrations of coronene with receptor **4c** revealed binding constants of 362 ± 4 M^{-1} in $CDCl_3$ and 444 ± 5 M^{-1} in CD_2Cl_2 after fitting to 1 : 1 binding isotherms. The supramolecular complex could also be characterized in the gas phase by HRMS and MS/MS analysis. In

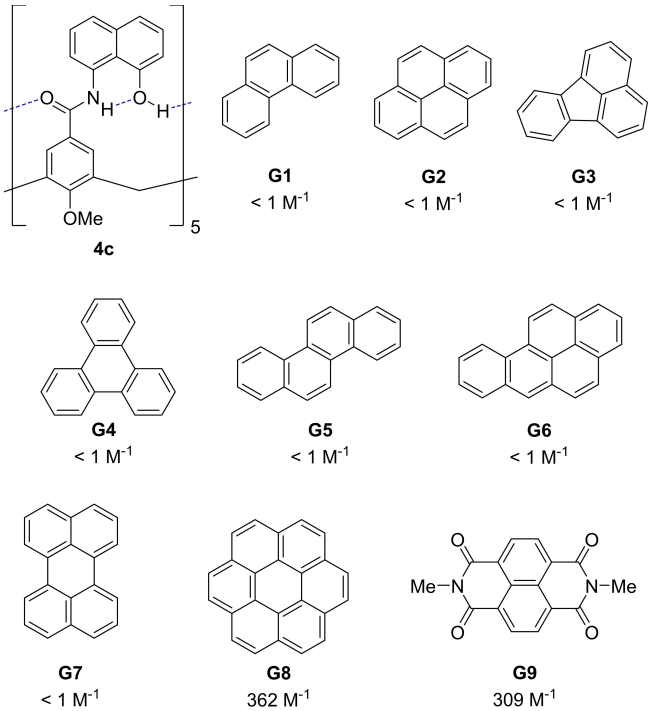

Figure 3. PAH compounds studied as guests for receptor **4c**. Association constants (K_a) in $CDCl_3$ are indicated.

order to assess the importance of the linkage of the upper aromatic panels in the supramolecular association, a comparable titration study was performed with receptor **4d** (Scheme 2), showing absence of binding and evidencing the influence of the hydrogen bond stabilization in the molecular recognition event. For the case of guest *N,N*-dimethylnaphthalenediimide (**G9**), analogous titrations with **4c** and data fitting revealed association constants of 309 ± 2 M^{-1} in $CDCl_3$ and 299 ± 3 M^{-1} in CD_2Cl_2. Interestingly, the difference in binding between pyrene (**G2**) and *N,N*-dimethylnaphthalenediimide (**G9**) appears to arise from molecular discrimination governed by electronic effects between host and guest – arguably more significant for binding that size and shape complementarity – as both molecules have similar volume. Although the binding constants may overall seem modest compared to other synthetic receptors of PAHs reported in literature,[23] the highly competitive nature of $CDCl_3$ and CD_2Cl_2 on binding needs to be emphasized – the stabilization of PAHs inside the cavitand needs to overcome a favorable solvent association with the host. Interestingly, the guest exchange process is fast in the ^1H NMR time scale as observed during the titrations experiments of **4c**, indicating that guest exchange occurs without unfolding of the cone conformation of the cavitand as opposed to what is observed with **R4A** derived cavitands.[12] This observation confirms that the non-covalent linkage of the receptor, although dynamic and flexible, is exceptionally robust, and the cavitand is able to release the bound guest without significantly altering its vase shape.

All the outstanding features discovered for receptor **4c** set the basis for the design and preparation of next generation cavitands, focusing on the ability of such hosts to adapt their conformation to the shape of their guests. The new receptors' design should match the aforementioned structural specifications, being the non-covalent linkage between the amide and naphthol groups on the upper rim essential for binding. As evidenced for the case of molecular discrimination between **G2** and **G9**, electronic complementarity has a massive impact on binding inside the cavity. Therefore, novel receptors based on **C5A** bearing electron deficient or electron rich walls may arise as promising modifications to finely tune the final properties of the cavitand.

3.3. Attempts to Diversify the 1,8-Aminonaphthol Panel

In light of the previous examinations, we aimed at synthetizing a new family of receptors with modified aromatic walls. To do so, we resorted to well-established aromatic transformations that could easily introduce functional groups to our elemental 1,8-aminonaphtol scaffold. With the tuning of the upper panels, we essentially sought for an impact on binding properties by increasing the electronic compatibility with the guests, and also to influence the acidity of the protons involved in the sewing resulting in a stronger panel linkage and overall stabilization of the cone shape. A first direct derivatization of cavitand **4c** was attempted by Friedel-Crafts acylation using acetyl chloride and aluminum trichloride in toluene (Scheme 3a). Unfortunately, monitoring of the reaction revealed a complex mixture of non-identified products. Considering the far from efficient multi-step reaction sequence leading to receptor **4c**, this approach was rapidly discarded, making the initial functionalization of the 1,8-aminonaphthol moiety and further coupling with the **C5A** core a more feasible strategy. On this regard, direct transformations on the readily available 1,8-aminonaphthol moiety were tested (Scheme 3b), resulting in either decomposition or intractable mixtures. These transformations involved direct S_EAr reactions on the already substituted naphthalene core, in order to introduce either halogens (bromide, fluoride) or carbonyl electron withdrawing groups (–CHO, $–COCH_2COOEt$) under various reaction conditions reported in literature. Zinc-mediated Friedel Crafts-type reaction using ethyl cyanoacetate in acid organic media did not lead to the desired adduct resulting in a more electron deficient naphthalene panel. Direct Duff formylation of 1,8-aminonaphthol using TFA or acetic acid also resulted unsuccessful. Considering the low stability of the 1,8-aminonaphthol core, arguably due to the electron rich nature of its substitution pattern, we decided to explore alternative synthetic approaches towards the same target panel (Scheme 3c). We shifted our strategy towards a late-stage formation of the *peri* amino-hydroxy substitution in the naphthalene scaffold, introducing beforehand the desired electron withdrawing functionalities. Thus, we foresaw that nitro analogues could be effective synthons enabling the

Israel Journal of Chemistry

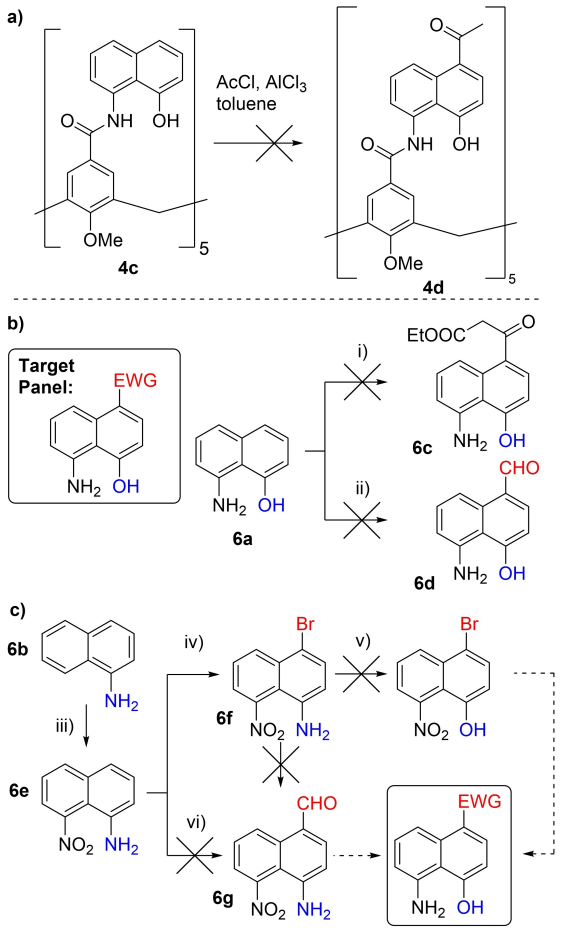

i) Ethyl cyanoacetate, $ZnCl_2$, HCl 4M, dioxane; ii) HMTA, TFA / AcOH. iii) HNO_3, H_2SO_4; iv) NBS, DCM; v) $NaNO_2$, H_2SO_4, $CuSO_4{\cdot}5H_2O$, Cu_2O, H_2O; or $NaNO_2$, H_2SO_4, H_2O, DMF; or $NaNO_2$, HBF_4, $CuSO_4{\cdot}5H_2O$, Cu_2O, H_2O. vi) $CuCl_2$, $2H_2O$, DMSO, HCl; or $POCl_3$, DMF; or ethyl formate, $ZnCl_2$, toluene.

Scheme 3. Strategies tested to further functionalize the 1,8-aminonaphthol panel.

synthesis of the targeted panel. Nitration of commercially available 1-naphthylamine using standard methods provided a mixture of separable 8-nitro-1-napthylamine and 5-nitro-1-napthylamine. The 1,8-isomer **6e** was subsequently regioselectively brominated using *N*-bromosuccinimide. Unfortunately, attempts to convert the amino group into the desired hydroxyl function via the diazonium salt resulted ineffective. Alternatively, we attempted the direct formylation of 8-nitro-1-naphtylamine in order to install an aldehyde group prior to the hydroxylation step. Unfortunately, none of the three methods tested allowed the isolation of the desired compound. Finally, lithiation of nitronatphthylamine bromide **6f** and trapping of the aryllithium with DMF was attempted, to no avail.

It remains elusive why the *peri* substituted amino-hydroxy naphthalene resulted so challenging to modify, but work is in progress to access electron rich and deficient aromatic naphthalene panels bearing the crucial functionalities for the hydrogen bonding linkage. In the meantime, our group explored alternative scaffolds coupled to **C5A** core in order to provide novel characteristics to the artificial synthetic receptors.

4. Second Generation Cavitands

In light of the hurdles encountered for the diversification of our 1st generation cavitand **4c**, we started exploring alternative scaffolds to the 1,8-aminonaphthol panel. We reasoned that 2-(aminomethyl)phenols (i.e. benzylamines with an *ortho*-hydroxy substituent), having the same spatial arrangement of phenol and amino groups, would be an interesting choice for a number of reasons. First, both the starting benzylamines and the resulting amides are expected to be far more stable than the corresponding highly electron rich 1,8-aminonaphthol derivatives. Additionally, the requested benzylamine building blocks are far easier to synthesize and offer greater prospects for structure diversification. And last, but not least, the introduction of an sp^3 carbon opened the door to accessing chiral panels and hence chiral cavitands.

4.1. Cavitand Derived from an Achiral Benzylamine Panel (8)

Based on these premises, we set out to synthesize cavitand **8** as a proof-of-concept structure. Cavitand **8** was easily prepared in one step from the common **C5A** pentaacid precursor **5c** and benzylamine **9** (Scheme 4). We chose **9** as a building block

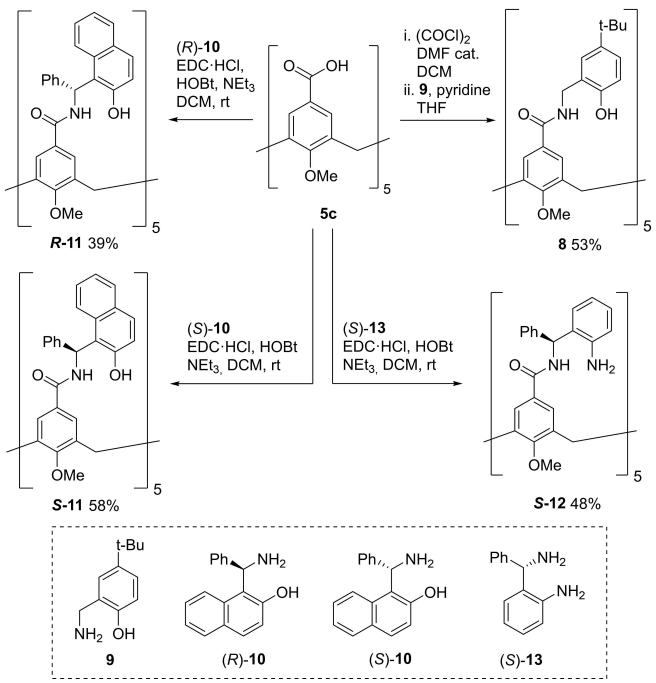

Scheme 4. Synthesis of cavitands **8**, **11**, and **12**. Inset: building blocks for the cavitands' upper panels (**9**, **10**, **13**).

because of its straightforward synthetic access. We also envisaged that the *tert*-butyl groups would become useful for isolation and purification purposes, and for solubilization in low polarity organic solvents that do not compete for hydrogen bonds. The ^{1}H NMR spectrum of cavitand **8** in $CDCl_3$ (298 K) lacked the features characteristic of slow conformational exchange observed for **4a** and **4c**, i.e. both the methylene (green/blue square) and the aromatic protons of the **C5A** core in **8** appeared as single resonances (Figure 2c). These signals were broad, suggesting that hydrogen bonding interactions would be operating to some extent, but low temperature experiments did not reveal any significant changes in the spectrum. This lack of preorganization and kinetic stability was attributed to the fact that the 2-(amidomethyl)phenol panel has a higher degree of conformational flexibility than the 1,8-amidonapthol panel, since an additional bond with free rotation is introduced. We next assessed the binding of commercially available PAHs with **9**, but no significant shifts could be observed at all during ^{1}H NMR titration experiments. These results point at very low association constants below the 1 M^{-1} threshold. These results showcase the delicate balance between preorganization and intrinsic flexibility of a host. We next sought to address the lack of preorganization of **8** by fine tuning the conformational mobility of the upper panels through steric effects. Eventually, we realized that the most effective way to do so would be adding substituents at the benzylic positions of these panels, thereby fulfilling our original goal of introducing chirality in the cavitand structure.

4.2. Cavitand Derived from a Chiral Benzylamine Panel: the Betti Cavitand (11)

MD simulations (Section 5) revealed that cavitand **4c** exists as an ensemble of low symmetry cone-like conformers, offering good prospects for developing chiral adaptable confined spaces based on the **C5A** scaffold. Such hosts would have the potential of surpassing the enantioselective molecular recognition capabilities of existing chiral self-folding cavitands based on **R4A**, in which transfer of chirality to the confined spaced is hampered by the rigid and highly symmetrical cavity.[24] During the design process of a chiral cavitand scaffold based on substitution at the benzylic positions of **8**, two main challenges had to be addressed. First, a chiral benzylamine building block accessible in optically pure form would be required, in order to avoid the formation of diasteromeric cavitand structures upon incorporation of the five chiral panels required. And second, even if the first condition was met, the resulting cavitands would have the potential to exist in two *cyclodiastereomeric* forms under slow exchange regime, resulting from the directional arrangement (clockwise or anticlockwise) of the hydrogen bond seam stabilizing the cone conformer ensemble (Scheme 5). Based on molecular modelling studies, our hypothesis was that sufficiently bulky substituents at the benzylic position would favor exclusively the *cyclodiasteromer* with these groups facing outward from the cavity, since they would clash in the opposite directional arrangement. After a brief literature survey for known homochiral (diaryl)methanamines that could be used as building blocks for our purpose, we focused our attention on the so-called Betti base (**10**), featuring the required aminophenol motif (Scheme 4).[25] This chiral amine is easily prepared in one step from 2-naphthol and benzaldehyde, and an efficient resolution process that yields multigram quantities of both enantiomers in excellent enantiomeric excess has been reported.[26] The corresponding diastereomerically pure enantiomeric cavitands cavitands (*R*,*R*,*R*,*R*)-**11** and (*S*,*S*,*S*,*S*)-**11** (abbreviated ***R*-11** and ***S*-11**) were obtained by coupling of pentaacid precursor **5c** with either enantiomer of **10** (Scheme 4).[13a] In this case, an amide coupling reagent combination was used, delivering the corresponding cavitands in good yields in a practical way. Remarkably, cavitand **11**

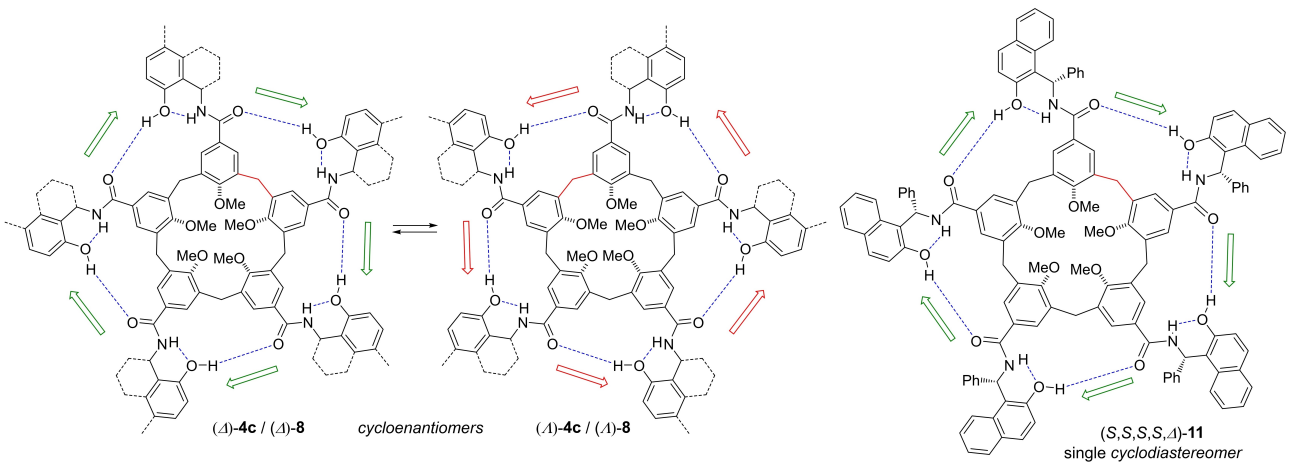

Scheme 5. Cavitands **4c** and **8** occur in two *cycloenantiomeric* forms in equilibrium, originating from directional arrangement of the hydrogen bond seam. Chiral cavitand **11** exists as a single *cyclodiastereomer.*

proved to be significantly more stable than its predecessors **4a/4c** both in the solid state and in solution, offering great prospects for further development and testing with this type of cavitand scaffold. Gratifyingly, the introduction of chirality at the benzylic position allowed the re-emergence of slow exchange behavior in **11**, as previously observed for cavitands **4a/4c** (Figure 2d). Both the H_a/H_b and the H_c/H_d protons appeared as separate resonances in $CDCl_3$, CD_2Cl_2 and C_6D_6, indicating slow inversion of the **C5A** core and slow rotation of the aromatic panel about the aryl-CONH- bond, relative to the NMR time scale. Additionally, only one set of signals was observed, confirming that the directionality of the hydrogen bond seam was fixed by the newly introduced stereogenic elements. It is remarkable that the addition of steric bulk at the benzylic position of the panels results in such a dramatic change in the fluxional behavior of the cavitand, when considering that cavitand **8** was in fast exchange regime under the same conditions.

For cavitand **11**, the barrier to self-exchange could be again ascertained by EXSY experiments, and a barrier of 17.7 kcal mol^{-1} was obtained in $CDCl_3$ at 298 K, which is close to the value obtained for cavitand **4c**. It is worth noting that the restraints imposed by the chiral panels imply that the motion sampled in the ^{1}H NMR spectra of **11** involves concerted inversion of the **C5A** core and panel rotation, linking two cavitand arrangements with the exact same Euclidean properties (Figure 2d). In order to assess the enantioselective molecular recognition capabilities of **11**, we assessed the binding constants of a series of chiral quaternary ammonium salts with ***R*-11** and ***S*-11** (Figure 4). Cavitand **11** provided enantioselective discrimination for most of the guests tested, and a remarkable K_R/K_S ratio of 1 : 18.7 was obtained for guest (*R*)-**G12**, the highest so far reported for enantioselective molecular recognition of quaternary ammonium salts.[27] These notable results indicate that the chiral panels efficiently shape a chiral environment in the confined space and showcase the benefit of having a flexible, contrasting with previous attempts of developing enantioselective molecular recognition with chiral hosts derived from either **R4A**[24] or **C5A**.[28]

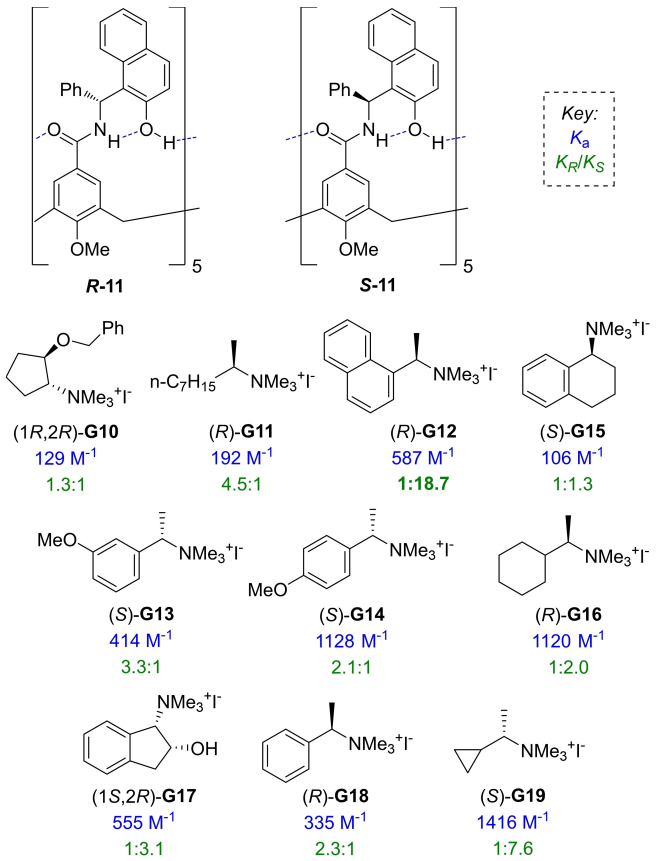

Figure 4. Chiral ammonium salts studied as guests for chiral cavitand **11**. Indicated below each guest are the highest association constant in $CDCl_3$ (K_a, blue) and the K_R/K_S diastereomeric ratio (green).

4.3. Testing the Limits of Cavitand Preorganization

Having established the validity of our chiral cavitand design and taking advantage of the improved chemical stability displayed by cavitands derived from benzylic amines, we set out to test the limits of the hydrogen bond stabilizing motif. We wondered whether substitution of the OH groups by NH_2 groups in the aromatic panels of cavitands similar to **11** would have a significant effect on the kinetic stabilization of the cone conformers. Even though anilines are in general significantly weaker hydrogen bond donors than phenols, we hypothesized whether the cooperative nature of the hydrogen bond network previously demonstrated in **4a/4c** and **11** could compensate an a priori unfavorable energetic balance. Besides a fundamental interest to strengthen the understanding of our self-folding cavitand scaffold, the introduction of NH_2 would be desirable for establishing polar interactions with guests present in the cavity through the free hydrogen not participating of the hydrogen bond seam in each NH_2 group. Thereby, we synthesized cavitand (*S*,*S*,*S*,*S*,*S*)-**12** (***S*-12**) following our previously established protocol, using readily available chiral amine (*S*)-**13** as a building block (Scheme 4).[29] In analogy to what was previously observed for **8**, the ^{1}H NMR spectrum of **12** in $CDCl_3$ presented the characteristic features of fast exchange between different conformers, including fast inversion of the **C5A** core (Figure 2e). As a result, we can conclude that introducing good hydrogen bond donors/acceptors in the design of **C5A** self-folding cavitands is important to access preorganized receptors. For the case of **12**, the intermolecular interaction between aniline and *N*-methylbenzamide can be used as a reference for the putative interaction bridging the cavitand walls (Scheme 6).[22] In this case, the calculated thermodynamic stabilization is only of 1.4 kcal mol^{-1}, in contrast to the value of 9.6 kcal mol^{-1} found for the model system of **4a/4c** (Scheme 1). These calculations provide a useful reference for further development of **C5A** derived self-

Israel Journal of Chemistry

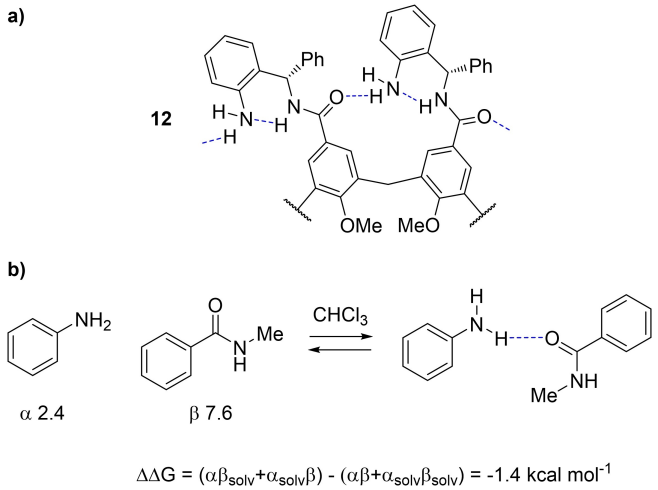

Scheme 6. a) Envisaged hydrogen bonding scheme for cavitand **12**, and b) thermodynamic balance of the model intermolecular interaction.

folding cavitands, since the thermodynamics of intermolecular interactions mimicking the key hydrogen bond interactions across cavitand panels are well correlated with the kinetic stabilization of the resulting cavitands in pre-organized cone conformers.

5. Conformational Analysis: MD Simulations

From early stages of this project, it became obvious that molecular modelling of the systems herein discussed based solely on the study of stationary points (obtained by DFT or other methods) would not be very useful. Computing the potential energy surface minima of cavitands derived from **R4A** is useful to gauge the host guest properties of such systems, because their intrinsic conformational rigidity makes the vase conformer responsible for binding a very stable arrangement even *in vacuo*. On the other hand, the optimization of **C5A** derived cavitands by semiempirical or DFT methods led to the collapse of the confined space to reduce the formation of voids, a process enabled by the increased flexibility of **C5A** derived structures. While these collapsed structures can be useful to guess the preferred conformational minima of the receptors, we reasoned that a meaningful modelling of the cavitands' behavior in solution would require sampling of multiple conformers in the presence of explicit solvent or suitable guests, and therefore resorted to MD simulations as the method of choice. The MD simulations of cavitands **4c** and **11** reveal that these hosts easily fluctuate between irregularly shaped cone conformers while preserving the integrity of the stabilizing hydrogen bond seam (Figure 5, panels b and c).

These transitions are fast, giving rise to the time averaged C_5 symmetry observed in the corresponding ^{1}H NMR spectra. On the contrary, we did not observe the inversion process or "cone flip" of the **C5A** core during the timespan of these simulations (between 0.5 and 1 μs). This is in good agreement

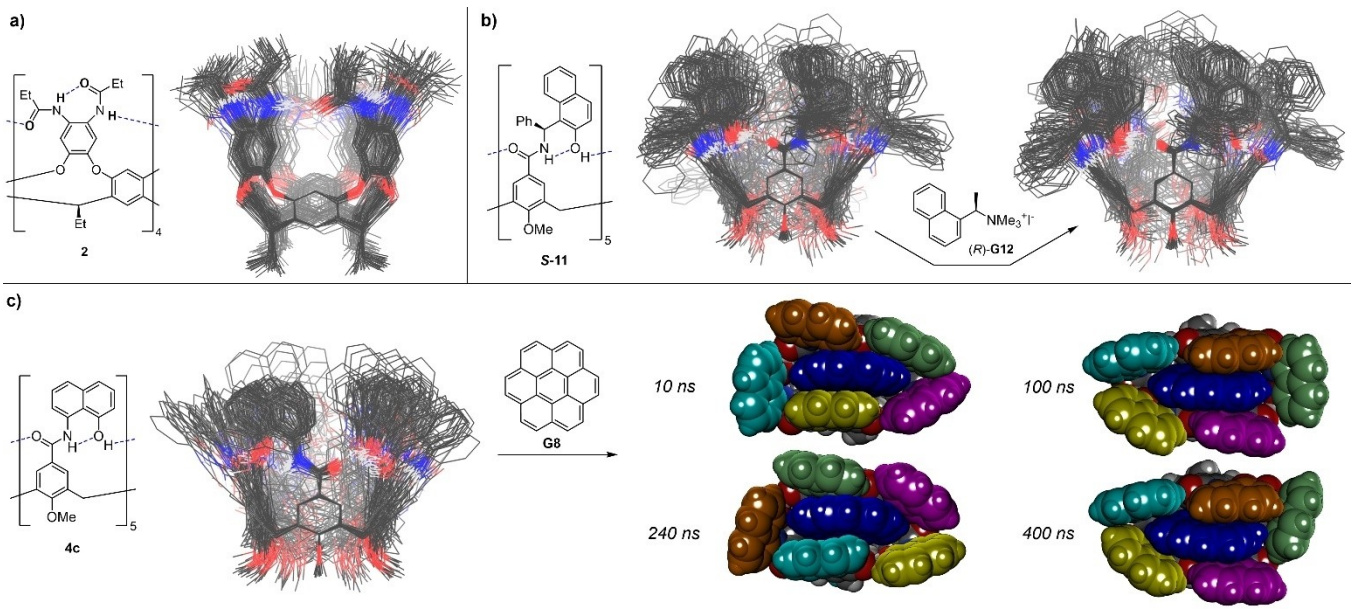

Figure 5. MD simulations (0.5 μs) of cavitands **2**, ***S*-11**, **4c**. a) **2** in $CHCl_3$, structure alignment at 20 ns intervals. b) ***S*-11** in $CHCl_3$ alone (left) and with ammonium salt (*R*)-**G12** as a guest; structure alignments at 20 ns intervals. c) **4c** in $CHCl_3$, structure alignment at 20 ns intervals (left), and snapshots of **4c** with bound coronene (**G8**, blue). The upper naphthalene panels of **4c** are color coded to highlight the fluxional behavior of the cavitand. Non-polar hydrogens are omitted for clarity in the overlaid structures.

with the high barriers calculated by EXSY NMR experiments, and the fact that such a process requires the disruption of the hydrogen bond seam. The MD simulations are useful to compare the flexibility of the **C5A** derived self-folding cavitands to that of the original **R4A** derived cavitands. Figure 5 displays the superposition of structures extracted from the MD trajectories, aligned by one of the aromatic rings of the **R4A** or **C5A** core. The resulting images quite eloquently reveal the rigidity of the **R4A** system in comparison to the new cavitands (Figure 5a). The MD simulations of cavitands **4c** and **11** in the presence of suitable guests illustrate their superior induced fit behavior.

The flexibility of the receptor allows it to adapt to the shape of the bound guest, maximizing the attractive non-covalent interactions that stabilize the host-guest complex. This is clearly observed in snapshots of the trajectory of **4c** with bound coronene (**G8**), showing how the receptor fluctuates among different conformers while keeping close π–π stacking interactions with the guest (Figure 5c). On the other hand, comparison between the MD trajectories of **11** in pure solvent and in the presence of a guest ((*R*)-**G12**) suggest a reduction of the conformational space to populate the conformers best fitting the shape of the bound guest (Figure 5b). This qualitative observation certainly deserves a more quantitative conformational analysis in future studies. Finally, the MD simulations also allowed sampling the guest exchange mechanism on some occasions. For the complexes of cavitand **4c** with PAH guests displaying no apparent binding in titration experiments (e. g. perylene, **G7**), the release of the guest into solution can be sampled during 0.5 μs trajectories. In this process, the guest slips away from the cavity and is replaced by solvent molecules without disruption of the stabilizing hydrogen bond seam. This interesting mode of action is complementary to the exchange mechanism in **R4A** derived hosts, which requires previous unfolding into (partially) open structures, resulting in higher barriers for guest exchange.[12]

6. Outlook

To sum up, we have developed a new family of self-folding cavitands based on calix[5]arene (**C5A**) that is one step closer to reproducing the complex dynamic behavior of biological receptors, and hence the unique functions underpinned by this fluxionality. Building up on the seminal concepts developed by pioneers of calixarene and cavitand chemistry, we have developed structures that are both genuinely flexible and pre-organized for binding. A key element of these systems is the replacement of covalent restraints by a carefully designed cooperative hydrogen bond stabilization motif. The construction of these receptors is based on joining building blocks through amide bonds, making the new cavitand scaffold a versatile platform for further diversification. The proof-of-concept systems developed so far bode good prospects for applications in PAH sequestration and supramolecular (enantioselective) catalysis, albeit some challenges remain to be addressed. Firstly, stable analogues of the 1,8-aminonaphthol core need to be synthesized, as well as structurally diverse and homochiral panels based on the 2-aminomethylphenol moiety. Wider and more spherical shapes can be accessed by using free hydroxyl groups at the lower rim of the cavitand, which necessitates of suitable protection schemes. On the other hand, the newfound flexibility of the **C5A** derived cavitands poses additional challenges to developing meaningful applications. Competitive binding of solvent molecules is significant in the new systems, making it difficult to quantify association constants. Additionally, the rational design of tailored host-guest systems is also far from trivial, and will necessitate of quantitative binding models based on advanced MD simulations methods. Such methods would also be helpful to distinguish the subtle differences between induced fit and conformational selection phenomena in our systems, and provide a good understanding of the guest exchange process at the molecular level. Work along these lines is underway in our group and will be published in due course.

Acknowledgements

We are grateful for financial support from grants PID2020-113181GB–I00 and TED2021-130573B–I00 funded by MCIN/AEI/ 10.13039/501100011033 and by the European Union NextGenerationEU/PRTR. We thank AGAUR/Generalitat de Catalunya for funding (2021SGR623) and for a predoctoral fellowship to R. L. (2020 FI_B 00132). Open Access funding provided thanks to the CRUE-CSIC agreement with Wiley.

References

[1] a) J.-M. Lehn, *Angew. Chem. Int. Ed.* **1988**, *27*, 89–112; b) D. J. Cram, *Angew. Chem. Int. Ed.* **1988**, *27*, 1009–1020.
[2] a) G. Montà-González, F. Sancenón, R. Martínez-Máñez, V. Martí-Centelles, *Chem. Rev.* **2022**, *122*, 13636–13708; b) F. Hof, S. L. Craig, C. Nuckolls, J. J. Rebek, *Angew. Chem. Int. Ed.* **2002**, *41*, 1488–1508.
[3] a) A. Ikeda, S. Shinkai, *Chem. Rev.* **1997**, *97*, 1713–1734; b) C. D. Gutsche, *Acc. Chem. Res.* **1983**, *16*, 161–170.
[4] C. Gropp, B. L. Quigley, F. Diederich, *J. Am. Chem. Soc.* **2018**, *140*, 2705–2717.
[5] J. R. Moran, S. Karbach, D. J. Cram, *J. Am. Chem. Soc.* **1982**, *104*, 5826–5828.
[6] a) M. Petroselli, Y.-Q. Chen, J. J. Rebek, Y. Yu, *Green Synthesis and Catalysis* **2021**, *2*, 123–130; b) B. W. Purse, J. Rebek, *Proc. Natl. Acad. Sci. USA* **2005**, *102*, 10777–10782; c) R. Pinalli, M. Suman, E. Dalcanale, *Eur. J. Org. Chem.* **2004**, *2004*, 451–462.
[7] J. R. Moran, J. L. Ericson, E. Dalcanale, J. A. Bryant, C. B. Knobler, D. J. Cram, *J. Am. Chem. Soc.* **1991**, *113*, 5707–5714.
[8] a) D. M. Rudkevich, G. Hilmersson, J. Rebek, *J. Am. Chem. Soc.* **1998**, *120*, 12216–12225; b) D. M. Rudkevich, G. Hilmersson, J. Rebek, *J. Am. Chem. Soc.* **1997**, *119*, 9911–9912.
[9] a) A. Lledó, A. Soler, *Org. Chem. Front.* **2017**, *4*, 1244–1249; b) F. R. Pinacho Crisóstomo, A. Lledó, S. R. Shenoy, T. Iwasawa,

J. Rebek, *J. Am. Chem. Soc.* **2009**, *131*, 7402–7410; c) R. J. Hooley, J. Rebek Jr, *Chem. Biol.* **2009**, *16*, 255–264; d) T. Iwasawa, R. J. Hooley, J. Rebek, *Science* **2007**, *317*, 493; e) K. Henzler-Wildman, D. Kern, *Nature* **2007**, *450*, 964–972.

[10] a) D. Ringe, G. A. Petsko, *Science* **2008**, *320*, 1428–1429; b) D. E. Koshland Jr, *Angew. Chem. Int. Ed.* **1995**, *33*, 2375–2378; c) B. Ma, S. Kumar, C.-J. Tsai, R. Nussinov, *Protein Eng. Des. Sel.* **1999**, *12*, 713–720.

[11] a) A. Lledó, J. Rebek Jr, *Chem. Commun.* **2010**, *46*, 1637–1639; b) T. Haino, D. M. Rudkevich, A. Shivanyuk, K. Rissanen, J. J. Rebek, *Chem. Eur. J.* **2000**, *6*, 3797–3805.

[12] R. López-Coll, R. Álvarez-Yebra, F. Feixas, A. Lledó, *Chem. Eur. J.* **2021**, *27*, 10099–10106.

[13] a) R. Álvarez-Yebra, R. López-Coll, P. Galán-Masferrer, A. Lledó, *Org. Lett.* **2023**; b) D. Lozano, R. Álvarez-Yebra, R. López-Coll, A. Lledó, *Chem. Sci.* **2019**, *10*, 10351–10355.

[14] a) M. Frei, F. Diederich, R. Tremont, T. Rodriguez, L. Echegoyen, *Helv. Chim. Acta* **2006**, *89*, 2040–2057; b) F. C. Tucci, D. M. Rudkevich, J. Rebek, *J. Org. Chem.* **1999**, *64*, 4555–4559.

[15] a) M. Chwastek, A. Szumna, *Org. Lett.* **2020**, *22*, 6838–6841; b) C. Naumann, E. Román, C. Peinador, T. Ren, B. O. Patrick, A. E. Kaifer, J. C. Sherman, *Chem. Eur. J.* **2001**, *7*, 1637–1645; c) H. Konishi, T. Nakamura, K. Ohata, K. Kobayashi, O. Morikawa, *Tetrahedron Lett.* **1996**, *37*, 7383–7386.

[16] a) H. Dvořáková, J. Štursa, M. Čajan, J. Moravcová, *Eur. J. Org. Chem.* **2006**, *2006*, 4519–4527; b) J. Stursa, H. Dvorakova, J. Smidrkal, H. Petrickova, J. Moravcova, *Tetrahedron Lett.* **2004**, *45*, 2043–2046.

[17] a) J. Pfeuffer-Rooschüz, S. Heim, A. Prescimone, K. Tiefenbacher, *Angew. Chem. Int. Ed.* **2022**, *61*, e202209885; b) J. Pfeuffer-Rooschüz, L. Schmid, A. Prescimone, K. Tiefenbacher, *JACS Au* **2021**, *1*, 1885–1891.

[18] D. R. Stewart, C. D. Gutsche, *Org. Prep. Proced. Int.* **1993**, *25*, 137–139.

[19] a) C. D. Gutsche, L. J. Bauer, *J. Am. Chem. Soc.* **1985**, *107*, 6052–6059; b) D. R. Stewart, M. Krawiec, R. P. Kashyap, W. H. Watson, C. D. Gutsche, *J. Am. Chem. Soc.* **1995**, *117*, 586–601.

[20] J. Garcia-Hartjes, S. Bernardi, C. A. G. M. Weijers, T. Wennekes, M. Gilbert, F. Sansone, A. Casnati, H. Zuilhof, *Org. Biomol. Chem.* **2013**, *11*, 4340–4349.

[21] L. Wang, C. W. Barth, M. Sibrian-Vazquez, J. O. Escobedo, M. Lowry, J. Muschler, H. Li, S. L. Gibbs, R. M. Strongin, *ACS Omega* **2017**, *2*, 154–163.

[22] M. C. Storer, C. A. Hunter, *Chem. Soc. Rev.* **2022**, *51*, 10064–10082.

[23] a) S. Ibáñez, E. Peris, *Angew. Chem. Int. Ed.* **2019**, *58*, 6693–6697; b) J. Samanta, R. Natarajan, *Org. Lett.* **2016**, *18*, 3394–3397; c) E. J. Dale, N. A. Vermeulen, A. A. Thomas, J. C. Barnes, M. Juríček, A. K. Blackburn, N. L. Strutt, A. A. Sarjeant, C. L. Stern, S. E. Denmark, J. F. Stoddart, *J. Am. Chem. Soc.* **2014**, *136*, 10669–10682; d) J. C. Barnes, M. Juríček, N. L. Strutt, M. Frasconi, S. Sampath, M. A. Giesener, P. L. McGrier, C. J. Bruns, C. L. Stern, A. A. Sarjeant, J. F. Stoddart, *J. Am. Chem. Soc.* **2013**, *135*, 183–192.

[24] E. Mann, J. Rebek, *Tetrahedron* **2008**, *64*, 8484–8487.

[25] M. Betti, *Org. Synth.* **1929**, *9*, 60.

[26] Y. Dong, R. Li, J. Lu, X. Xu, X. Wang, Y. Hu, *J. Org. Chem.* **2005**, *70*, 8617–8620.

[27] a) X.-N. Han, P.-F. Li, Y. Han, C.-F. Chen, *Angew. Chem. Int. Ed.* **2022**, *61*, e202202527; b) S. J. Nemat, H. Jędrzejewska, A. Prescimone, A. Szumna, K. Tiefenbacher, *Org. Lett.* **2020**, *22*, 5506–5510; c) H. Chai, Z. Chen, S.-H. Wang, M. Quan, L.-P. Yang, H. Ke, W. Jiang, *CCS Chem* **2020**, *2*, 440–452; d) G.-W. Zhang, P.-F. Li, Z. Meng, H.-X. Wang, Y. Han, C.-F. Chen, *Angew. Chem. Int. Ed.* **2016**, *55*, 5304–5308..

[28] T. Haino, H. Fukuoka, H. Iwamoto, Y. Fukazawa, *Supramol. Chem.* **2008**, *20*, 51–57.

[29] a) X. Zhong, G. Xiao, W. Zhou, *Synlett* **2021**, *32*, 1019–1023; b) P. L. Anderson, W. J. Houlihan, P. K. Kapa, A. Kucerovy, P. G. Mattner, (Sandoz Ltd.), EP0564397 A1, **1993**.

Manuscript received: May 15, 2023
Revised manuscript received: June 19, 2023
Version of record online: July 6, 2023

REVIEW

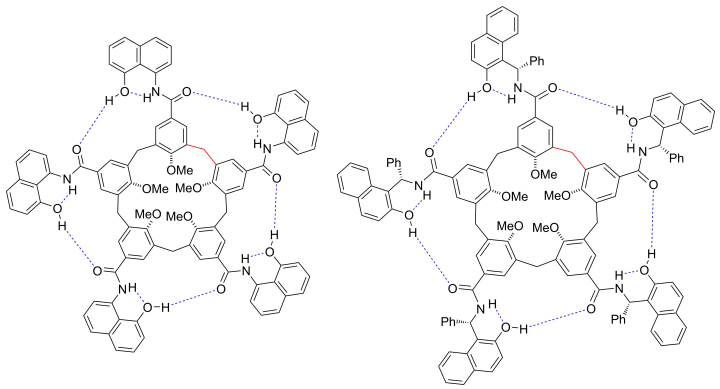

R. Álvarez-Yebra, R. López-Coll, N. Clos-Garrido, Dr. D. Lozano, Dr. A. Lledó**